Laser irradiance scaling in polar direct drive implosions on the National Ignition Facility

T. J. Murphy, N. S. Krasheninnikova, G. A. Kyrala, P. A. Bradley, J. A. Baumgaertel, J. A. Cobble, P. Hakel, S. C. Hsu, J. L. Kline, D. S. Montgomery, K. A. D. Obrey, R. C. Shah, I. L. Tregillis, M. J. Schmitt, R. J. Kanzleiter, S. H. Batha, R. J. Wallace, S. D. Bhandarkar, P. Fitzsimmons, M. L. Hoppe, A. Nikroo, M. Hohenberger, P. W. McKenty, H. G. Rinderknecht, M. J. Rosenberg, and R. D. Petrasso

Articles you may be interested in

The effect of laser spot shapes on polar-direct-drive implosions on the National Ignition Facility
Phys. Plasmas **22**, 032701 (2015); 10.1063/1.4913988

Mode 1 drive asymmetry in inertial confinement fusion implosions on the National Ignition Facility
Phys. Plasmas **21**, 042702 (2014); 10.1063/1.4870390

Radiative shocks produced from spherical cryogenic implosions at the National Ignition Facilitya)
Phys. Plasmas **20**, 056315 (2013); 10.1063/1.4805081

Polar direct drive: Proof-of-principle experiments on OMEGA and prospects for ignition on the National Ignition Facilitya)
Phys. Plasmas **12**, 056304 (2005); 10.1063/1.1876252

Polar direct drive on the National Ignition Facility
Phys. Plasmas **11**, 2763 (2004); 10.1063/1.1689665

Laser irradiance scaling in polar direct drive implosions on the National Ignition Facility

T. J. Murphy,[1,a)] N. S. Krasheninnikova,[1] G. A. Kyrala,[1] P. A. Bradley,[1] J. A. Baumgaertel,[1] J. A. Cobble,[1] P. Hakel,[1] S. C. Hsu,[1] J. L. Kline,[1] D. S. Montgomery,[1] K. A. D. Obrey,[1] R. C. Shah,[1] I. L. Tregillis,[1] M. J. Schmitt,[1] R. J. Kanzleiter,[1] S. H. Batha,[1] R. J. Wallace,[2] S. D. Bhandarkar,[2] P. Fitzsimmons,[3] M. L. Hoppe,[3] A. Nikroo,[3,b)] M. Hohenberger,[4] P. W. McKenty,[4] H. G. Rinderknecht,[5] M. J. Rosenberg,[5,c)] and R. D. Petrasso[5]

[1]*Los Alamos National Laboratory, P.O. Box 1663, Los Alamos, New Mexico 87545, USA*
[2]*Lawrence Livermore National Laboratory, 7000 East Ave., Livermore, California 94550, USA*
[3]*General Atomics, P.O. Box 85608, San Diego, California 92186, USA*
[4]*University of Rochester Laboratory for Laser Energetics, 250 E. River Rd., Rochester, New York 14623, USA*
[5]*Plasma Science and Fusion Center, Massachusetts Institute of Technology, Cambridge, Massachusetts 02139, USA*

Polar-direct-drive experiments conducted at the National Ignition Facility [E. I. Moses, Fusion Sci. Technol. **54**, 361 (2008)] performed at laser irradiance between 1 and $2 \times 10^{15} \, \mathrm{W/cm^2}$ exhibit increased hard x-ray emission, decreased neutron yield, and reduced areal density as the irradiance is increased. Experimental x-ray images at the higher irradiances show x-ray emission at the equator, as well as degraded symmetry, that is not predicted in hydrodynamic simulations using flux-limited energy transport, but that appear when non-local electron transport together with a model to account for cross beam energy transfer (CBET) is utilized. The reduction in laser power for equatorial beams required in the simulations to reproduce the effects of CBET on the observed symmetry also reproduces the yield degradation consistent with experimental data. © 2015 AIP Publishing LLC. [http://dx.doi.org/10.1063/1.4931092]

I. INTRODUCTION

The goal of inertial confinement fusion[1] (ICF) is to achieve thermonuclear ignition and burn of deuterium and tritium fusion fuel. This is to be done by compressing a capsule containing the fuel to the state where the temperature and density are sufficiently high to achieve alpha-particle heating and self-sustained burn. The effort to achieve thermonuclear ignition in the laboratory using high energy lasers is being pursued using two main approaches. The first, using the indirect drive method,[2] utilizes x rays generated by heating the inside of a high-Z cavity in which a capsule of fusion fuel is located. The National Ignition Facility (NIF) laser[3] was built for this purpose, and the effort to achieve ignition in this manner is ongoing.[4] In the second method, the lasers directly illuminate the capsule.[5] This method is usually performed using nearly spherically symmetric illumination of the beams on the capsule.[6] The location of the beams on the National Ignition Facility precludes symmetric direct illumination. Consequently, the pointing of the NIF beams is steered off-center in a configuration called polar direct drive[7,8] (PDD) that has been used to achieve symmetric implosions on both OMEGA[9–13] and on NIF.[14–17]

The potential advantages of direct drive, including the use of simple, capsule-only targets, and the ability to apply the full available laser energy directly to the capsule, led to the choice of the PDD configuration for a series of experiments[18] designed[13] to study the effects of the mix of shell material into the fuel on implosion performance[19] for validation of simulations. In these experiments, NIF was utilized at the maximum allowed laser power[20] in a short (~2 ns) square pulse to produce an irradiance of ~$2 \times 10^{15} \, \mathrm{W/cm^2}$ in order to drive the implosion with a strong shock and attain high temperature and neutron yield.

In the initial PDD plastic capsule experiments,[18] oblate symmetry ($P_2/P_0 \sim 30\%$ at the time of peak neutron emission) together with an equatorial enhanced emission feature were observed. While the symmetry was typical of PDD implosions, the enhanced equatorial emission was not observed on similar experiments[12] performed on the Omega laser facility[6] at lower irradiance (~$0.8 \times 10^{15} \, \mathrm{W/cm^2}$). In an attempt to improve the implosion symmetry on a subsequent NIF shot, the polar laser illumination was reduced. While the symmetry indeed improved, this change also resulted in a more prominent equatorial feature. Since this platform was being developed to study the effects of an equatorial defect on mix,[19] the equatorial emission feature had the potential to mask the effect that was to be measured. The NIF experiments were being performed at over twice the irradiance of the OMEGA experiments, and since strong hard x ray emission from the equatorial region was observed on the NIF experiments and not on OMEGA experiments, one hypothesis[18] proposed was that the bright band of self-emission around the capsule's equator was caused by nonlinear laser-plasma interactions (LPIs).

a)Electronic mail: tjmurphy@lanl.gov
b)Present address: Lawrence Livermore National Laboratory, 7000 East Ave., Livermore, California 94550, USA.
c)Present address: University of Rochester Laboratory for Laser Energetics, 250 E. River Rd., Rochester, New York 14623, USA.

TABLE I. Parameters and results of the experiments used in this irradiance scan.

	Low	Medium	High
Energy on capsule (kJ)	319	462	607
Irradiance (10^{15} W/cm^2)	1.0	1.4	1.9
Neutron yield (10^{11} neutrons)	7.2 ± 0.2	5.9 ± 0.2	3.7 ± 0.2
Neutron bang Time (ns)	3.80 ± 0.20	3.24 ± 0.10	3.04 ± 0.07
X ray bang Time (ns)	3.87 ± 0.07	3.44 ± 0.08	3.27 ± 0.01
Ion temperature (keV)	3.66 ± 0.16	3.71 ± 0.16	3.37 ± 0.24
Hot spot radius (μm)	130 ± 5	145 ± 5	180 ± 5
Fuel ρR (mg/cm^2)	11.1 ± 1.1	7.4 ± 0.7	5.6 ± 0.5

II. EXPERIMENTS

Since LPI effects correlate strongly with laser intensity, to test the hypothesis that the equatorial feature was due to LPI and to quantify the threshold irradiance of this effect, PDD implosions were performed on NIF at three different laser energies (Table I). The targets (Fig. 1) consisted of plastic shells with a nominal diameter of 2200 μm and thickness of 42 μm. The inner 2 μm of the shells was doped with 2.1% by atom germanium, and a 2-μm thick layer buried by 5 μm was doped with 1.9% by atom gallium to allow diagnosis of mix and shell temperature through x-ray spectroscopy.[21] The capsules were mounted on a glass fill tube, which also served as the mounting stalk. The fill tube had a diameter of 30 μm at the point that it entered the capsule. The capsules were filled with 5 atm of deuterium at shot time.

The high energy experiment utilized 46 quads (a quad is a 2-by-2 array of NIF beams), with the two remaining quads directed at a backlighter foil. In this case, the other quads in
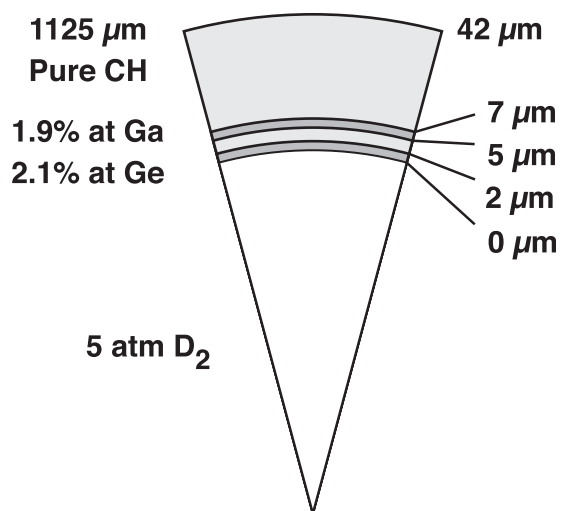

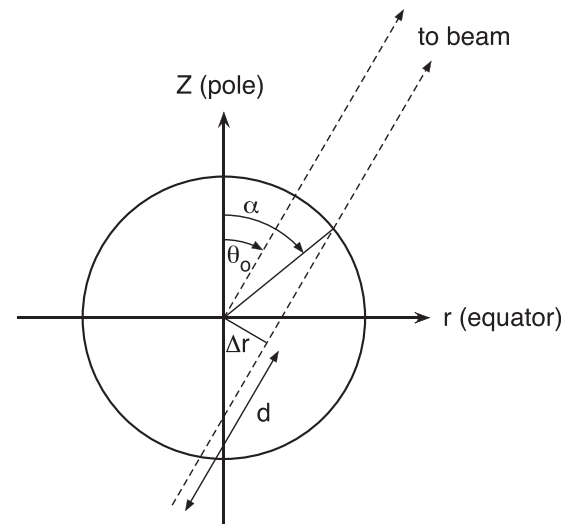FIG. 1. "Pie diagram" of the capsules used for these experiments.

FIG. 2. Coordinates used[22] to specify the pointing. θ_o is the angle between the polar axis and the direction to the center of the quad of beams. α is the polar angle of the location on the capsule surface to which the beams are pointed after a displacement of Δr. d is the defocus applied after this displacement to improve illumination uniformity.

the ring from which the backlighter beams were taken were azimuthally repositioned in an attempt to symmetrize the drive in their absence.[22] For the low and medium energy experiments, the capsules were illuminated with all 48 of the NIF quads.

The laser drive consisted of a square pulse with a width at half maximum of 2.15 ns and a rise time of approximately 150 ps. Beams were pointed[22] (Fig. 2) to provide optimum simulated PDD implosion symmetry (Table II). Laser power in beams located 23° and 30° from the poles of the target chamber was reduced to nominally 80% of the power of those in the 44.5° and 50° cones in an effort to further symmetrize the implosion (Fig. 3).

The capsules were imaged using gated x-ray pinhole cameras[24] located on the upper pole of the target chamber and on the equator at a location 160° azimuthally displaced from the position where the fill tube entered the capsule. The images were filtered using 275 μm of polyimide, filtering out most emission at x-ray energies less than about 4 keV. Implosion images were obtained over a period of 800 ps with a gate time of about 90 ps.

X-ray bang times were measured using a streak camera[25] located near the upper pole of the target chamber. Neutron bang times were obtained using a particle time-of-flight system[26] mounted on the x-ray camera pointed at the equator.

TABLE II. Beam pointing used for these experiments. Pointing parameters are defined in Figure 2. Laser wavelengths are prior to frequency tripling. For the 44.5° quad, A and B refer to the two beams closer to the pole, and C and D to the beams closer to the equator.

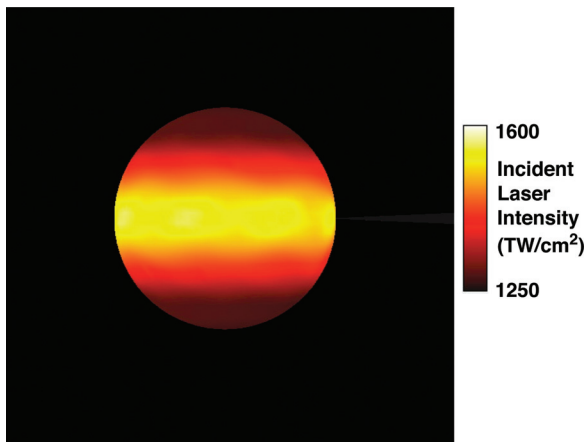| Quad: θ_o	23.5°	30.0°	44.5° A and B	44.5° C and D	50.0°
α	31.3°	37.8°	42.2°	79.9°	83.0°
Defocus (mm)	18	19	24	16	12
λ(nm)	1053.24	1053.09	1052.43	1052.43	1052.43

FIG. 3. Laser irradiance on the capsule calculated with the VisRad code.[23] Polar beams are reduced to nominally 80% of the power of the equatorial beams since they are closer to normal incidence and were expected to couple better to the capsule than the equatorial beams.

Equatorial view images (Fig. 4) reveal a band of emission along the capsule equator for the two higher irradiances. This band is similar to that seen previously[18] on similar implosions. When the band is present, it is seen at the beginning of capsule self emission, up to 500 ps prior to x-ray bang time for the high irradiance case. The band persists during the self emission and moves inward with the capsule surface as the implosion proceeds. The disappearance of the

equatorial band at low irradiance supports the hypothesis that some LPI effect is responsible for the band.

In addition to the appearance of equatorial emission at high irradiance, the generation of hot electrons increases and the performance of the implosion decreases with increasing irradiance.

Hot electrons (Fig. 5) inferred from high-energy x-ray emission from the target as measured by a filter fluorescer system (FFLEX)[27] are observed to increase by a factor of 5.6 for an increase in laser irradiance of 1.9. These hot electrons are generally attributed to two-plasmon decay.[17] A time-integrated hard-x-ray imager[28] located on the equator provided images of the implosions in x rays with energy greater than 25 keV (Fig. 6), allowing localization of the area where the high-energy x-ray emission is originating. The increased intensity of these images with increasing laser drive is consistent with the FFLEX data. The location of the brightest hard-x-ray emission is at the equator of the capsule, in the region of highest laser irradiance and most oblique beam incidence on the capsule, suggesting that hot electrons are being generated in this region.

The performance of the capsules is observed to decrease with increasing irradiance. In particular, the neutron yield (Fig. 7) from the $D + D \rightarrow n + {}^3He$ reaction was lower in shots with higher laser drive, while the observed ion temperature remains nearly constant. The observed decrease in yield without a corresponding decrease in ion temperature can be attributed to decreased capsule compression at higher irradiance. This is seen both as an increase in the radius of the x ray hot spot and a decrease in the fuel areal density (ρR) at neutron bang time. Fuel ρR can be determined[30,31] by comparing the secondary reaction yields of neutrons from the burn up of fusion-produced tritons and protons from fusion-produced ${}^3He$. The ratio of the final to initial ρR is equal to the square of the convergence, allowing the volume and average density at bang time to be calculated.

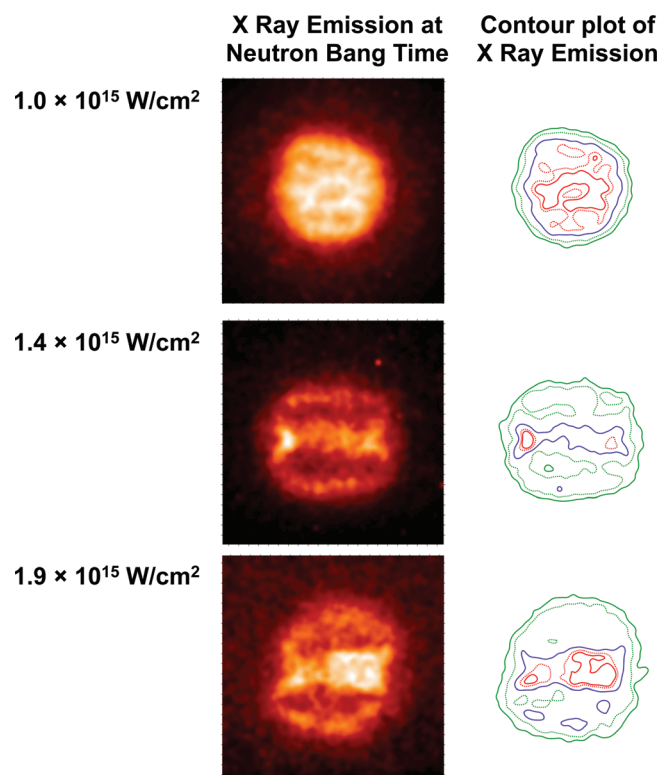The effect of the decreased compression on the yield can be approximated using

FIG. 4. Equatorial images of the x-ray emission at the time of peak neutron emission (Table I) and contour plots of the 20% (solid green), 30% (dashed green), 50% (solid blue) 70% (dashed red), and 80% (solid red) x-ray emission contours. The 50% contour highlights the equatorial band for the two higher irradiance images. Each image is 500 μm on a side and the color scale has been normalized. The fill tube enters from the back of the capsule and the polar axis is vertical in these images.
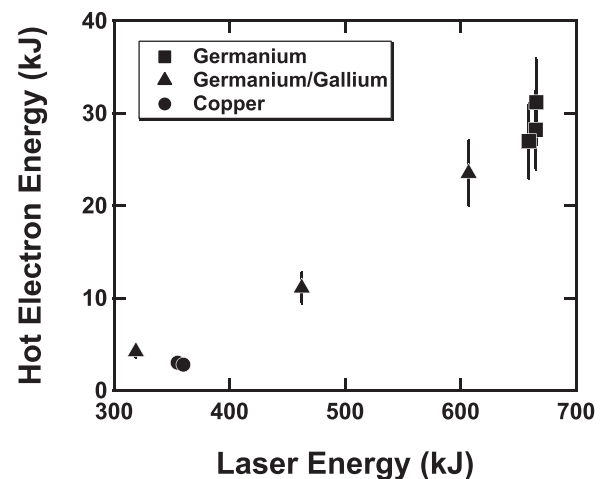

FIG. 5. The energy in hot electrons, as inferred from the hard x-ray flux, increased with increasing laser energy, while the temperature stayed constant at 58 ± 3 keV. Shown are experiments described in this work (triangles) along with those from previous experiments[18] (squares) using only germanium dopant and subsequent experiments[29] (circles), which used copper dopant.

1.0 × 10^{15} W/cm^2   **1.4 × 10^{15} W/cm^2**   **1.9 × 10^{15} W/cm^2**
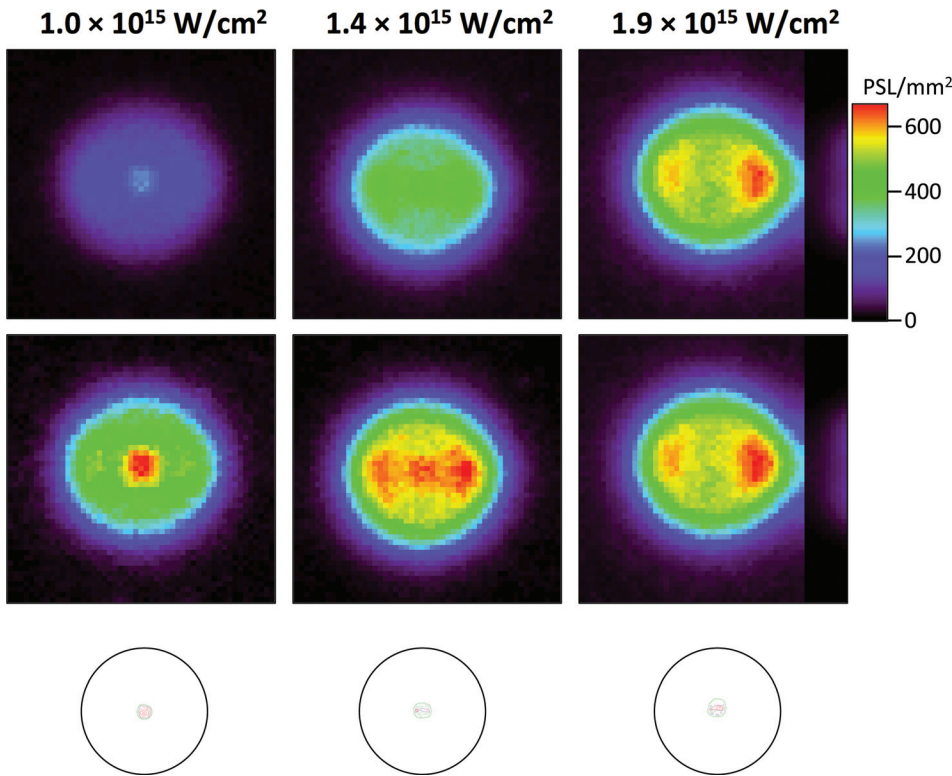

FIG. 6. Time-integrated images of the implosions measured in x rays with energy above about 25 keV measured using the hard-x-ray imager.[28] Images on the upper row are on the same color scale, while those in the middle row are normalized to show the change in the location of high-energy x ray emission, suggesting that hot electrons are created near the equator in the higher laser intensity implosions. The bottom row shows the initial diameter of the capsule, along with the x-ray contours from Figure 4. Images are approximately 4700 μm on each slide. The polar axis is vertical in these images.

$$Y_{dd} = \frac{1}{2} n_d^2 \langle \sigma v \rangle V_f \tau, \tag{1}$$

where n_d is the deuterium number density at bang time, V_f is the compressed volume of the fuel, $\langle \sigma v \rangle$ is the reaction rate at the burn-averaged ion temperature, and τ is the duration of the burn. The compressed deuterium density is related to the initial density through $n_d = n_{d,i} V_i / V_f$. The reaction rate for the DD fusion reaction[32] varies with ion temperature as about $T_i^{3.5}$ in the region of 3 to 4 keV and can be approximated as $\langle \sigma v \rangle (T_i) = \langle \sigma v \rangle (3.5 \, \text{keV})(T_i/3.5 \, \text{keV})^{3.5}$. Thus, the yield can be expected to vary with $T_i^{3.5} V_i^2 / V_f$. The final volume can be estimated using the 20% x-ray emission contour from Figure 4 as the extent of the hot spot or by using the convergence determined from the measured fuel ρR. The ion

temperatures are measured.[33] It is seen that the measured yield is consistent with this scaling (Fig. 8). For the scaling in Figure 8, the only free parameter was the burn duration, which was taken as 250 ± 50 ps. Thus, at the higher laser
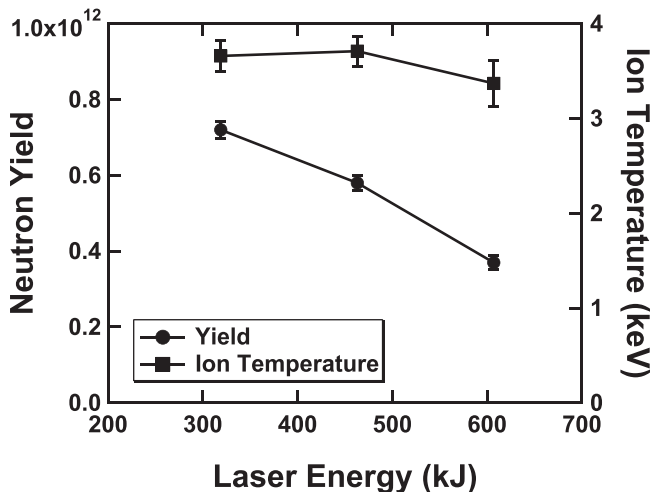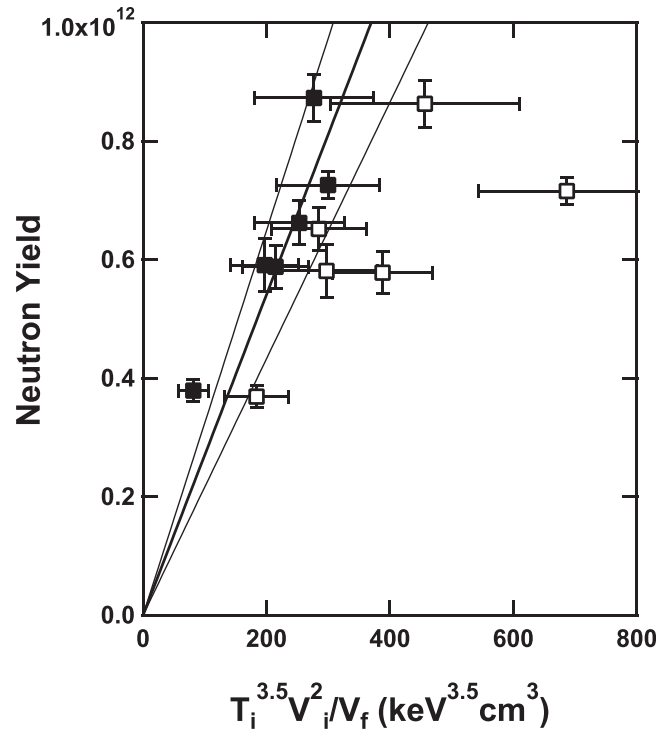

FIG. 8. Neutron yield scales with ion temperature to the 3.5 power, and inversely with the volume of the hot spot, as determined by the 20% contour of x-ray emission at peak neutron emission time (filled squares) or by comparing the initial and final fuel areal densities (open squares). The expected scaling is shown as the solid lines, using a burn duration of 250 ± 50 ps. Data from the three experiments described in this paper, as well as others shown in Fig. 5, are included.

FIG. 7. Neutron yield was observed to decrease with increasing laser energy, while the observed ion temperature remained nearly constant.

irradiances, the efficiency of heating and compressing the fuel is reduced, resulting in lower neutron yields, even though in these experiments there was no corresponding decrease in ion temperature.

III. COMPARISON WITH SIMULATIONS

Calculations performed prior to the experiments with the radiation-hydrodynamics code HYDRA[34] using a flux-limited energy transport model (with a flux limiter of $f = 0.06$) do not show the equatorial emission feature. Instead, the simulations (Fig. 9(a)) show reduced emission from the equator, with otherwise good spherical symmetry. Performing the simulations with a nonlocal electron transport (NLET) model[35] produces a strong equatorial feature (Fig. 9(b)) due to the heat flux reduction in the polar direction. However, the addition of the NLET model also changes

the symmetry of the implosion from oblate to very prolate, which was not observed in the experiment.

In these implosions, cross beam energy transfer[36,37] (CBET) is expected[16] to occur, leading to a reduction in the effective equatorial laser drive of approximately 30%. Simulations of polar direct drive experiments designed for ignition relevance[17] have had success in reproducing implosion symmetry by utilizing both NLET and CBET. The HYDRA code does not currently have a CBET model that is applicable to direct drive implosions, so its effect was included by either modifying the power split between equatorial and polar beams or by reducing the power on the equatorial beams. Figure 9(c) shows a simulated image when the polar and equatorial beam powers are set equal to each other. This image reproduces the shape of the equatorial emission feature seen in the data but misses the overall implosion shape. Reducing the power in the 44.5° C and D (the two beams closest to the equator in these quads) and the 50.0°
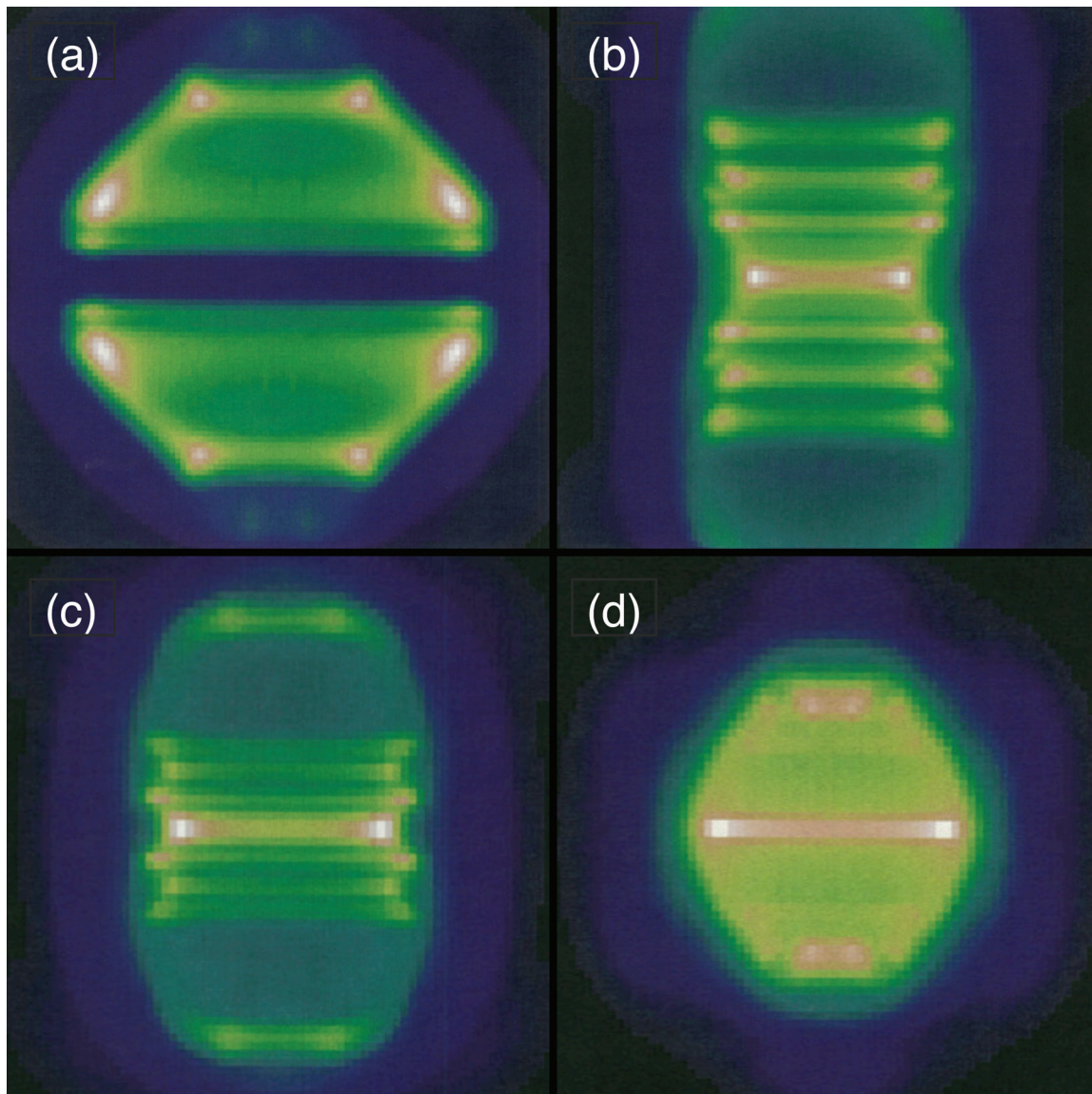

FIG. 9. Post-shot simulated self-emission images using (a) flux-limited energy transport (f = 0.06), (b) HYDRA's non-local electron transport (NLET), (c) NLET with energy redistributed to simulate cross-beam energy transfer so that polar and equatorial beams contain the same energy, and (d) NLET with 30% of the energy removed from the 44.5° C and D and the 50.0° beams to simulate cross-beam energy transfer. Images are $400\,\mu$m on a side and are at about 3.2 ns after the start of the laser pulse except (d), which is at 3.4 ns. The polar axis is vertical in these images.

beams by 30% (Fig. 9(d)) comes closer to reproducing the symmetry of the implosion seen in the experiments, but with changes in the structure and 200 ps delay of the appearance of the self-emission band.

Figure 10 shows the measured asymmetry as a function of time for three different irradiances. Also shown is the asymmetry of the simulated implosion images at a time near peak x-ray emission for different reductions of laser power in the equatorial beams to simulate the effects of various levels of CBET for the medium and low irradiance experiments. The asymmetry is measured at the contour of emission equal to 20% of the peak x-ray emission in the images. At low irradiance, NLET and CBET are not needed in the simulation to match the measured symmetry, while at medium irradiance, NLET and an equatorial power reduction of 30% to model CBET are required. In the high-irradiance experiment, two quads were directed at a backlighter foil, and the remaining quads were repointed in azimuth to compensate. This created an inherently three-dimensional geometry, with beam crossing angles varying around the capsule. It was not considered practical to attempt to simulate the effects of CBET in this geometry.

The simulated asymmetry at 3.5 ns (near x-ray bang time) is plotted *vs* equatorial power reduction in Figure 11. The ellipse includes the simulation points that are consistent with the experimental asymmetry during a 0.2 ns period centered around 3.5 ns. The range of asymmetries is consistent with an equatorial power reduction of $33 \pm 5\%$.

Simulations show that the neutron yield decreases for these experiments as CBET increases (Fig. 12). Reducing
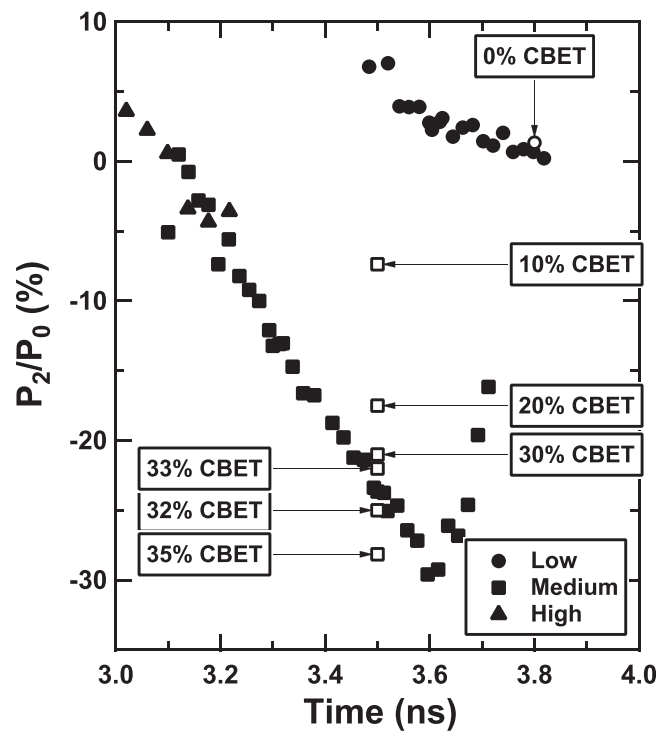

FIG. 11. Simulated P_2/P_0 at 3.5 ns as a function of the reduction in equatorial power used to simulate CBET for the medium irradiance shot. The ellipse is chosen to cover the range of experimental asymmetry at 3.5 ± 0.1 ns, and the simulated values for different equatorial power reductions, indicating a likely CBET range of $33 \pm 5\%$ for this case.

FIG. 10. Measured P_2/P_0 *vs* time for the low, medium, and high irradiance experiments, along with the symmetry at bang time simulated using different equatorial irradiance reductions. The symmetry of the low-irradiance experiment is consistent with simulations using flux-limited energy transport and no CBET model, while equatorial power reductions near 30% and NLET are needed to match the symmetry of the medium irradiance experiments near bang time.
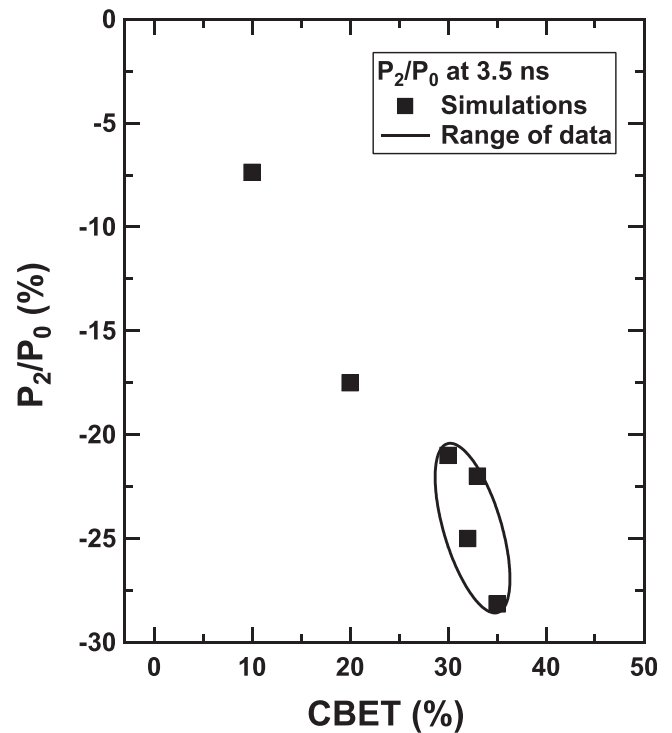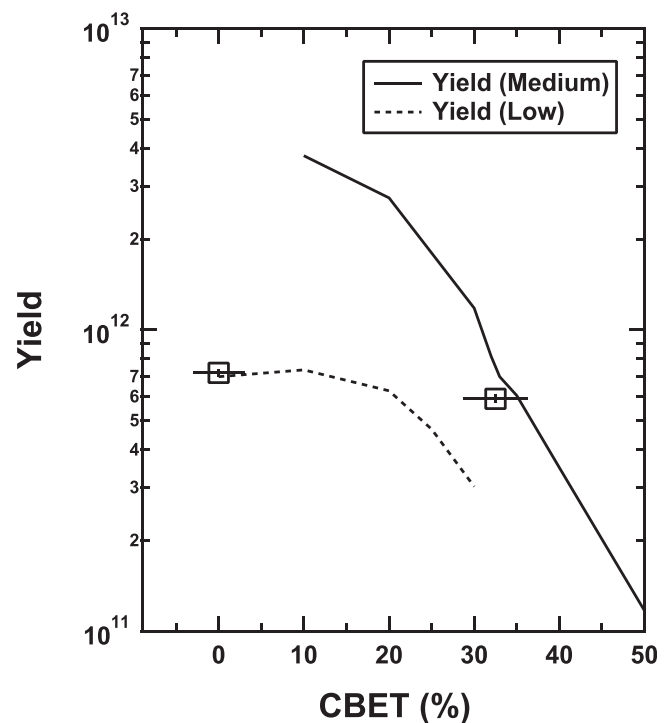

FIG. 12. Simulated neutron yield as a function of the reduction in equatorial power used to simulate CBET for the medium and low irradiance cases, with the measured neutron yield. The range of equatorial power reduction for the medium irradiance shot is taken from the ellipse in Figure 11, and that for the low irradiance case is taken as $0 \pm 5\%$ since the images were round, in agreement with design.

the equatorial power by the amount required to explain the measured asymmetry, we find that within the uncertainty, the simulations indicate that this level of power reduction is consistent with the experimental yields.

IV. CONCLUSIONS

Experiments utilizing polar direct drive on the National Ignition Facility at high irradiance demonstrate a decrease in capsule performance as irradiance increases, along with an increase in hot electron generation, which occurs near the equator where irradiance is the highest. The decrease in neutron yield is consistent with a decrease in the compression achieved. The effects of both non-local electron transport and cross beam energy transport must be included in simulations to reproduce the symmetry of the implosion. The magnitude of the equatorial irradiance reduction used to simulate the effect of CBET on implosion symmetry is consistent with the yield reduction seen in these experiments. An equatorial x-ray emission feature, observed in experiments, appears in simulations when non-local transport is included.

ACKNOWLEDGMENTS

[1]J. Nuckolls, L. Wood, A. Thiessen, and G. Zimmerman, Nature **239**, 139 (1972).

[2]J. D. Lindl, P. Amendt, R. L. Berger, S. G. Glendinning, S. H. Glenzer, S. W. Haan, R. L. Kauffman, O. L. Landen, and L. J. Suter, Phys. Plasmas **11**, 339 (2004).

[3]E. I. Moses, Fusion Sci. Technol. **54**, 361 (2008).

[4]J. D. Lindl, O. L. Landen, J. Edwards, E. I. Moses, J. Adams, P. A. Amendt, N. Antipa, P. A. Arnold, L. J. Atherton, S. Azevedo, D. Barker, M. A. Barrios, I. Bass, S. H. Baxamusa, R. Beeler, B. V. Beeman, P. M. Bell, L. R. Benedetti, L. Bernstein, L. Berzak Hopkins, S. D. Bhandarkar, T. Biesiada, R. M. Bionta, D. L. Bleuel, E. J. Bond, M. Borden, M. W. Bowers, D. K. Bradley, D. Browning, G. K. Brunton, J. Bude, S. C. Burkhart, R. F. Burr, B. Butlin, J. A. Caggiano, D. A. Callahan, A. C. Carpenter, C. W. Carr, D. T. Casey, C. Castro, J. Celeste, P. M. Celliers, C. J. Cerjan, J. Chang, M. Chiarappa-Zucca, C. Choate, T. J. Clancy, D. S. Clark, S. J. Cohen, G. W. Collins, A. Conder, J. R. Cox, P. S. Datte, G. A. Deis, E. L. Dewald, P. Di Nicola, J. M. Di Nicola, L. Divol, S. N. Dixit, T. Döppner, V. Draggoo, O. Drury, R. Dylla-Spears, E. G. Dzenitis, J. M. Dzenitis, M. J. Eckart, D. C. Eder, J. H. Eggert, R. B. Ehrlich, G. V. Erbert, J. Fair, D. R. Farley, M. Fedorov, B. Felker, R. Finucane, A. Fisher, D. N. Fittinghoff, J. Folta, R. J. Fortner, T. Frazier, G. Frieders, S. Frieders, S. Friedrich, J. Fry, J. Gaylord, S. M. Glenn, S. H. Glenzer, B. Golick, G. Gururangan, G. Guss, S. W. Haan, B. J. Haid, B. Hammel, A. V. Hamza, E. P. Hartouni, R. Hatarik, B. W. Hatch, S. P. Hatchett, R. Hawley, C. Haynam, J. Heebner, G. Heestand, M. R. Hermann, V. J. Hernandez, D. G. Hicks, D. E. Hinkel, D. D. Ho, J. P. Holder, D. Holunga, J. Honig, J. Horner, R. K. House, M. Hutton, N. Izumi, M. C. Jackson, K. S. Jancaitis, D. R. Jedlovec, M. A. Johnson, O. S. Jones, D. H. Kalantar, R. L. Kauffman, L. Kegelmeyer, G. Kerbel, M. Key, S. F. Khan, J. R. Kimbrough, R. Kirkwood, J. J. Klingman, J. A. Koch, T. R. Kohut, J. M. Koning, K. M. Knittel, B. J. Kozioziemski, G. W. Krauter, K. Krauter, A. Kritcher, J. Kroll, W. L. Kruer, G. LaCaille, K. N. LaFortune, L. J. Lagin, T. A. Land, A. B. Langdon, S. H. Langer, D. W. Larson, D. A. Latray, T. Laurence, S. LePape, R. A. Lerche, Z. Liao, J. Liebman, R. A. London, R. Lowe-Webb, T. Ma, B. J. MacGowan, A. J. MacKinnon, A. G. MacPhee, T. N. Malsbury, K. Manes, A. M. Manuel, E. R. Mapoles, M. M. Marinak, C. D. Marshall, D. Mason, N. Masters, D. G. Mathisen, I. Matthews, T. McCarville, J. M. McNaney, D. J. Meeker, N. B. Meezan, J. Menapace, P. Michel, P. E. Miller, J. L. Milovich, M. Mintz, R. Montesanti, M. Monticelli, J. D. Moody, M. J. Moran, J. C. Moreno, D. H. Munro, R. A. Negres, J. R. Nelson, M. Norton, M. Nostrand, M. O'Brien, Y. P. Opachich, C. Orth, A. E. Pak, E. S. Palma, J. N. E. Palmer, T. G. Parham, H.-S. Park, P. K. Patel, R. W. Patterson, J. E. Peterson, J. L. Peterson, T. Phillips, R. Prasad, K. Primdahl, S. T. Prisbrey, S. R. Qiu, J. E. Ralph, K. S. Raman, F. Ravizza, B. Raymond, B. A. Remington, M. A. Rever, J. Reynolds, M. J. Richardson, A. C. Riddle, B. Rittmann, M. D. Rosen, J. S. Ross, J. R. Rygg, R. A. Sacks, J. T. Salmon, J. D. Salmonson, J. D. Sater, R. L. Saunders, R. Sawicki, K. Schaffers, D. H. Schneider, M. B. Schneider, H. A. Scott, S. M. Sepke, R. Seugling, D. A. Shaughnessy, M. J. Shaw, R. Shelton, N. Shen, N. Shingleton, N. Simanovskaia, V. Smalyuk, D. A. Smauley, M. Spaeth, B. K. Spears, D. R. Speck, T. M. Spinka, P. T. Springer, M. Stadermann, W. Stoeffl, J. Stolken, C. Stolz, E. Storm, D. J. Strozzi, T. Suratwala, L. J. Suter, J. Taylor, C. A. Thomas, G. L. Tietbohl, R. Tommasini, D. Trummer, B. VanWonterghem, R. Von Rotz, R. J. Wallace, C. F. Walters, A. Wang, A. L. Warrick, S. Weaver, S. V. Weber, P. J. Wegner, K. Widmann, C. C. Widmayer, E. A. Williams, P. K. Whitman, K. Wilhelmsen, M. Witte, L. Wong, R. D. Wood, S. Yang, C. Yeamans, B. K. Young, B. Yoxall, R. A. Zacharias, G. B. Zimmerman, S. Batha, C. R. Danly, V. Fatherley, G. P. Grim, N. Guler, H. W. Herrmann, Y. Kim, J. L. Kline, G. A. Kyrala, R. J. Leeper, D. Martinson, F. E. Merrill, R. E. Olson, C. Wilde, M. D. Wilke, D. C. Wilson, G. A. Chandler, G. W. Cooper, K. D. Hahn, K. J. Peterson, C. L. Ruiz, K. C. Chen, N. Dorsano, M. Emerich, C. Gibson, D. Hoover, M. Hoppe, J. D. Kilkenny, K. Moreno, H. Wilkens, S. Woods, J. A. Frenje, M. G. Johnson, C. K. Li, R. D. Petrasso, H. Rinderknecht, M. Rosenberg, F. H. Séguin, A. Zylstra, W. Garbett, P. Graham, T. Guymer, A. S. Moore, J.-L. Bourgade, P. Gauthier, J.-P. Leidinger, L. Masse, F. Philippe, and R. H. H. Scott, Phys. Plasmas **21**, 129902 (2014).

[5]R. L. McCrory, D. D. Meyerhofer, R. Betti, R. S. Craxton, J. A. Delettrez, D. H. Edgell, V. Y. Glebov, V. N. Goncharov, D. R. Harding, D. W. Jacobs-Perkins, J. P. Knauer, F. J. Marshall, P. W. McKenty, P. B. Radha, S. P. Regan, T. C. Sangster, W. Seka, R. W. Short, S. Skupsky, V. A. Smalyuk, J. M. Soures, C. Stoeckl, B. Yaakobi, D. Shvarts, J. A. Frenje, C. K. Li, R. D. Petrasso, and F. H. Séguin, Phys. Plasmas **15**, 055503 (2008).

[6]T. R. Boehly, R. L. McCrory, C. P. Verdon, W. Seka, S. J. Loucks, A. Babushkin, R. E. Bahr, R. Boni, D. K. Bradley, R. S. Craxton, J. A. Delettrez, W. R. Donaldson, R. Epstein, D. Harding, P. A. Jaanimagi, S. D. Jacobs, K. Kearney, R. L. Keck, J. H. Kelly, T. J. Kessler, R. L. Kremens, J. P. Knauer, D. J. Lonobile, L. D. Lund, F. J. Marshall, P. W. McKenty, D. D. Meyerhofer, S. F. B. Morse, A. Okishev, S. Papernov, G. Pien, T. Safford, J. D. Schnittman, R. Short, M. J. Shoup III, M. Skeldon, S. Skupsky, A. W. Schmid, V. A. Smalyuk, D. J. Smith, J. M. Soures, M. Wittman, and B. Yaakobi, Fusion Eng. Des. **44**, 35 (1999).

[7]S. Skupsky, J. A. Marozas, R. S. Craxton, R. Betti, T. J. B. Collins, J. A. Delettrez, V. N. Goncharov, P. W. McKenty, P. B. Radha, T. R. Boehly, J. P. Knauer, F. J. Marshall, D. R. Harding, J. D. Kilkenny, D. D. Meyerhofer, T. C. Sangster, and R. L. McCrory, Phys. Plasmas **11**, 2763 (2004).

[8]G. A. Kyrala, N. Delamater, D. Wilson, J. Guzik, D. Haynes, M. Gunderson, K. Klare, R. W. Watt, W. M. Wood, and W. Varnum, Laser Part. Beams **23**, 187 (2005).

[9]R. S. Craxton, F. J. Marshall, M. J. Bonino, R. Epstein, P. W. McKenty, S. Skupsky, J. A. Delettrez, I. V. Igumenshchev, D. W. Jacobs-Perkins, J. P. Knauer, J. A. Marozas, P. B. Radha, and W. Seka, Phys. Plasmas **12**, 056304 (2005).

[10]J. A. Marozas, F. J. Marshall, R. S. Craxton, I. V. Igumenshchev, S. Skupsky, M. J. Bonino, T. J. B. Collins, R. Epstein, V. Y. Glebov, D. Jacobs-Perkins, J. P. Knauer, R. L. McCrory, P. W. McKenty, D. D. Meyerhofer, S. G. Noyes, P. B. Radha, T. C. Sangster, W. Seka, and V. A. Smalyuk, Phys. Plasmas **13**, 056311 (2006).

[11]P. B. Radha, J. A. Marozas, F. J. Marshall, A. Shvydky, T. J. B. Collins, V. N. Goncharov, R. L. McCrory, P. W. McKenty, D. D. Meyerhofer, T. C. Sangster, and S. Skupsky, Phys. Plasmas **19**, 082704 (2012).

[12]J. A. Cobble, T. J. Murphy, M. J. Schmitt, P. A. Bradley, N. S. Krashenninikova, K. A. Obrey, S. C. Hsu, I. L. Tregillis, G. R. Magelssen, F. J. Wysocki, and S. H. Batha, Phys. Plasmas **19**, 122713 (2012).

[13]N. S. Krasheninnikova, J. A. Cobble, T. J. Murphy, I. L. Tregillis, P. A. Bradley, P. Hakel, S. C. Hsu, G. A. Kyrala, K. A. Obrey, M. J. Schmitt, J. A. Baumgaertel, and S. H. Batha, Phys. Plasmas **21**, 042703 (2014).

[14]A. M. Cok, R. S. Craxton, and P. W. McKenty, Phys. Plasmas **15**, 082705 (2008).

[15]T. J. B. Collins, J. A. Marozas, K. S. Anderson, R. Betti, R. S. Craxton, J. A. Delettrez, V. N. Goncharov, D. R. Harding, F. J. Marshall, R. L. McCrory, D. D. Meyerhofer, P. W. McKenty, P. B. Radha, A. Shvydky, S. Skupsky, and J. D. Zuegel, Phys. Plasmas **19**, 056308 (2012).

[16]P. B. Radha, F. J. Marshall, J. A. Marozas, A. Shvydky, I. Gabalski, T. R. Boehly, T. J. B. Collins, R. S. Craxton, D. H. Edgell, R. Epstein, J. A. Frenje, D. H. Froula, V. N. Goncharov, M. Hohenberger, R. L. McCrory, P. W. McKenty, D. D. Meyerhofer, R. D. Petrasso, T. C. Sangster, and S. Skupsky, Phys. Plasmas **20**, 056306 (2013).

[17]M. Hohenberger, P. B. Radha, J. F. Myatt, S. LePape, J. A. Marozas, F. J. Marshall, D. T. Michel, S. P. Regan, W. Seka, A. Shvydky, T. C. Sangster, J. W. Bates, R. Betti, T. R. Boehly, M. J. Bonino, D. T. Casey, T. J. B. Collins, R. S. Craxton, J. A. Delettrez, D. H. Edgell, R. Epstein, G. Fiksel, P. Fitzsimmons, J. A. Frenje, D. H. Froula, V. N. Goncharov, D. R. Harding, D. H. Kalantar, M. Karasik, T. J. Kessler, J. D. Kilkenny, J. P. Knauer, C. Kurz, M. Lafon, K. N. LaFortune, B. J. MacGowan, A. J. Mackinnon, A. G. MacPhee, R. L. McCrory, P. W. McKenty, J. F. Meeker, D. D. Meyerhofer, S. R. Nagel, A. Nikroo, S. Obenschain, R. D. Petrasso, J. E. Ralph, H. G. Rinderknecht, M. J. Rosenberg, A. J. Schmitt, R. J. Wallace, J. Weaver, C. Widmayer, S. Skupsky, A. A. Solodov, C. Stoeckl, B. Yaakobi, and J. D. Zuegel, Phys. Plasmas **22**, 056308 (2015).

[18]M. J. Schmitt, P. A. Bradley, J. A. Cobble, J. R. Fincke, P. Hakel, S. C. Hsu, N. S. Krasheninnikova, G. A. Kyrala, G. R. Magelssen, D. S. Montgomery, T. J. Murphy, K. A. Obrey, R. C. Shah, I. L. Tregillis, J. A. Baumgaertel, F. J. Wysocki, S. H. Batha, R. S. Craxton, P. W. McKenty, P. Fitzsimmons, A. Nikroo, and R. Wallace, Phys. Plasmas **20**, 056310 (2013).

[19]P. A. Bradley, J. A. Cobble, I. L. Tregillis, M. J. Schmitt, K. D. Obrey, V. Glebov, S. H. Batha, G. R. Magelssen, J. R. Fincke, S. C. Hsu, N. S. Krasheninnikova, T. J. Murphy, and F. J. Wysocki, Phys. Plasmas **19**, 092703 (2012).

[20]C. A. Haynam, P. J. Wegner, J. M. Auerbach, M. W. Bowers, S. N. Dixit, G. V. Erbert, G. M. Heestand, M. A. Henesian, M. R. Hermann, K. S. Jancaitis, K. R. Manes, C. D. Marshall, N. C. Mehta, J. Menapace, E. Moses, J. R. Murray, M. C. Nostrand, C. D. Orth, R. Patterson, R. A. Sacks, M. J. Shaw, M. Spaeth, S. B. Sutton, W. H. Williams, C. C. Widmayer, R. K. White, S. T. Yang, and B. M. Van Wonterghem, Appl. Opt. **46**, 3276 (2007).

[21]P. Hakel, G. A. Kyrala, P. A. Bradley, N. S. Krasheninnikova, T. J. Murphy, M. J. Schmitt, I. L. Tregillis, R. J. Kanzleieter, S. H. Batha, C. J. Fontes, M. E. Sherrill, D. P. Kilcrease, and S. P. Regan, Phys. Plasmas **21**, 063306 (2014).

[22]N. S. Krasheninnikova, S. M. Finnegan, and M. J. Schmitt, Phys. Plasmas **19**, 012702 (2012).

[23]J. J. MacFarlane, J. Quantum Spect. Rad. Trans. **81**, 287 (2003).

[24]J. A. Oertel, R. Aragonez, T. Archuleta, C. Barnes, L. Casper, V. Fatherley, T. Heinrichs, R. King, D. Landers, F. Lopez, P. Sanchez, G. Sandoval, L. Schrank, and P. Walsh, Rev. Sci. Instrum. **77**, 10E308 (2006).

[25]S. F. Khan, P. M. Bell, D. K. Bradley, S. R. Burns, J. R. Celeste, L. S. Dauffy, M. J. Eckart, M. A. Gerhard, C. Hagmann, D. I. Headley, J. P. Holder, N. Izumi, M. C. Jones, J. W. Kellogg, H. Khater, J. R. Kimbrough, A. G. MacPhee, Y. P. Opachich, N. E. Palmer, R. B. Petre, J. L. Porter, R.

Shelton, T. L. Thomas, and J. B. Worden, Proc. SPIE **8505**, 850505 (2012).

[26]H. G. Rinderknecht, M. Gatu Johnson, A. B. Zylstra, N. Sinenian, M. J. Rosenberg, J. A. Frenje, C. J. Waugh, C. K. Li, F. H. Séguin, R. D. Petrasso, J. R. Rygg, J. R. Kimbrough, A. MacPhee, G. W. Collins, D. Hicks, A. Mackinnon, P. Bell, R. Bionta, T. Clancy, R. Zacharias, T. Döppner, H. S. Park, S. LePape, O. Landen, N. Meezan, E. I. Moses, V. U. Glebov, C. Stoeckl, T. C. Sangster, R. Olson, J. Kline, and J. Kilkenny, Rev. Sci. Instrum. **83**, 10D902 (2012).

[27]J. W. McDonald, R. L. Kauffman, J. R. Celeste, M. A. Rhodes, F. D. Lee, L. J. Suter, A. P. Lee, J. M. Foster, and G. Slark, Rev. Sci. Instrum. **75**, 3753 (2004).

[28]T. Döppner, C. A. Thomas, L. Divol, E. L. Dewald, P. M. Celliers, D. K. Bradley, D. A. Callahan, S. N. Dixit, J. A. Harte, S. M. Glenn, S. W. Haan, N. Izumi, G. A. Kyrala, G. LaCaille, J. K. Kline, W. L. Kruer, T. Ma, A. J. MacKinnon, J. M. McNaney, N. B. Meezan, H. F. Robey, J. D. Salmonson, L. J. Suter, G. B. Zimmerman, M. J. Edwards, B. J. MacGowan, J. D. Kilkenny, J. D. Lindl, B. M. Van Wonterghem, L. J. Atherton, E. I. Moses, S. H. Glenzer, and O. L. Landen, Phys. Rev. Lett. **108**, 135006 (2012).

[29]T. J. Murphy, G. A. Kyrala, N. S. Krasheninnikova, P. A. Bradley, J. A. Cobble, I. L. Tregillis, K. A. D. Obrey, J. A. Baumgaertel, S. C. Hsu, R. C. Shah, P. Hakel, J. L. Kline, M. J. Schmitt, R. J. Kanzleiter, S. H. Batha, R. J. Wallace, S. Bhandarkar, P. Fitzsimmons, M. Hoppe, A. Nikroo, and P. McKenty, "Development of a polar direct drive platform for mix and burn experiments on the National Ignition Facility" J. Phys.: Conf. Ser. (in press).

[30]H. Azechi, R. O. Stapf, N. Miyanaga, R. Tsuji, M. Yamanaka, S. Ido, K. Nishihara, T. Yabe, and C. Yamanaka, Phys. Rev. Lett. **59**, 2635 (1987).

[31]H. G. Rinderknecht, M. J. Rosenberg, A. B. Zylstra, B. Lahmann, F. H. Séguin, J. A. Frenje, C. K. Li, M. Gatu Johnson, R. D. Petrasso, L. Berzak Hopkins, J. Caggiano, L. Divol, E. Hartouni, R. Hatarik, S. Hatchett, S. LePape, A. Mackinnon, J. McNaney, N. Meezan, M. Moran, P. A. Bradley, J. L. Kline, N. S. Krasheninnikova, G. A. Kyrala, T. J. Murphy, M. J. Schmitt, I. L. Tregillis, S. H. Batha, J. Knauer, and J. Kilkenny, Phys. Plasmas **22**, 082709 (2015).

[32]H.-S. Bosch and G. M. Hale, Nucl. Fusion **32**, 611 (1992).

[33]V. Y. Glebov, T. C. Sangster, C. Stoeckl, J. P. Knauer, W. Theobald, K. L. Marshall, M. J. Shoup III, T. Buczek, M. Cruz, T. Duffy, M. Romanofsky, M. Fox, A. Pruyne, M. J. Moran, R. A. Lerche, J. McNaney, J. D. Kilkenny, M. J. Eckart, D. Schneider, D. Munro, W. Stoeffl, R. Zacharias, J. J. Haslam, T. Clancy, M. Yeoman, D. Warwas, C. J. Horsfield, J.-L. Bourgade, O. Landoas, L. Disdier, G. A. Chandler, and R. J. Leeper, Rev. Sci. Instrum. **81**, 10D325 (2010).

[34]M. M. Marinak, R. E. Tipton, O. L. Landen, T. J. Murphy, P. Amendt, S. W. Haan, S. P. Hatchett, C. J. Keane, R. McEachern, and R. Wallace, Phys. Plasmas **3**, 2070 (1996).

[35]G. P. Schurtz, P. D. Nicolaï, and M. Busquet, Phys. Plasmas **7**, 4238 (2000).

[36]I. V. Igumenshchev, D. H. Edgell, V. N. Goncharov, J. A. Delettrez, A. V. Maximov, J. F. Myatt, W. Seka, A. Shvydky, S. Skupsky, and C. Stoeckl, Phys. Plasmas **17**, 122708 (2010).

[37]I. V. Igumenshchev, W. Seka, D. H. Edgell, D. T. Michel, D. H. Froula, V. N. Goncharov, R. S. Craxton, L. Divol, R. Epstein, R. Follett, J. H. Kelly, T. Z. Kosc, A. V. Maximov, R. L. McCrory, D. D. Meyerhofer, P. Michel, J. F. Myatt, T. C. Sangster, A. Shvydky, S. Skupsky, and C. Stoeckl, Phys. Plasmas **19**, 056314 (2012).